Angle dependent Fiber Bragg grating inscription in microstructured polymer optical fibers

Bundalo, Ivan-Lazar; Nielsen, Kristian; Bang, Ole

Published in:
Optics Express

Link to article, DOI:
10.1364/OE.23.003699

Publication date:
2015

Document Version
Publisher's PDF, also known as Version of record

Angle dependent Fiber Bragg grating inscription in microstructured polymer optical fibers

Ivan-Lazar Bundalo,[1*] Kristian Nielsen[1] and Ole Bang[1]

[1]*DTU Fotonik, Department of Photonic Engineering, Technical University of Denmark, DK-2800 Kgs. Lnygby, Denmark*

**ivlab@fotonik.dtu.dk*

Abstract: We report on an incidence angle influence on inscription of the Fiber Bragg Gratings in Polymethyl methacrylate (PMMA) microstructured polymer optical fibers. We have shown experimentally that there is a strong preference of certain angles, labeled ΓK, over the other ones. Angles close to ΓK showed fast start of inscription, rapid inscription and stronger gratings. We have also shown that gratings can be obtained at almost any angle but their quality will be lower if they are not around ΓK angle. Our experimental results verify earlier numerical and experimental predictions of Marshall *et al.*

OCIS codes: (060.2370) Fiber optics sensors; (060.4005) Microstructured fibers; (350.2770) Gratings; (060.2270) Fiber characterization; (160.5470) Polymers; (060.3735) Fiber Bragg gratings.

References and links

1. A. D. Kersey, M. Davis, H. J. Patrick, M. LeBlanc, K. P. Koo, C. G. Askins, M. Putnam, and E. J. Friebele, "Fiber grating sensors," J. Lightwave Technol. **15**(8), 1442–1463 (1997).
2. K. O. Hill and G. Meltz, "Fiber Bragg Grating technology fundamentals and overview," **15**(8), 1263–1276 (1997).
3. K. Peters, "Polymer optical fiber sensors—a review," Smart Mater. Struct. **20**(1), 013002 (2011).
4. A. Cusano, A. Cutolo, and J. Albert, *Fiber Bragg Grating Sensors: Recent Advancements, Industrial Applications and Market Exploitation* (Bentham Science, 2009).
5. S. H. Law, M. A. van Eijkelenborg, G. W. Barton, C. Yan, R. Lwin, and J. Gan, "Cleaved end-face quality of microstructured polymer optical fibres," Opt. Commun. **265**(2), 513–520 (2006).
6. S. H. Law, J. D. Harvey, R. J. Kruhlak, M. Song, E. Wu, G. W. Barton, M. A. Van Eijkelenborg, and M. C. J. Large, "Cleaving of microstructured polymer optical fibres," Opt. Commun. **258**(2), 193–202 (2006).
7. A. Stefani, S. Andresen, W. Yuan, and O. Bang, "Dynamic characterization of polymer optical fibers," IEEE Sens. J. **12**(10), 3047–3053 (2012).
8. M. Large, G. W. Barton, L. Poladian, and M. A. van Eijkelenborg, *Microstructured Polymer Optical Fibre*, 1st ed. (Springer, 2008), p. 232.
9. K. Krebber, S. Liehr, and J. Witt, "Smart technical textiles based on fibre optic sensors," in *OFS2012 22nd International Conference on Optical Fiber Sensors, Invited Paper*, Y. Liao, W. Jin, D. D. Sampson, R. Yamauchi, Y. Chung, K. Nakamura, and Y. Rao, eds. (2012), Vol. 8421, p. 84212A–10.
10. A. Argyros, R. Lwin, S. G. Leon-Saval, J. Poulin, L. Poladian, and M. C. J. Large, "Low loss and temperature stable microstructured polymer optical fibers," J. Lightwave Technol. **30**(1), 192–197 (2012).
11. W. Yuan, L. Khan, D. J. Webb, K. Kalli, H. K. Rasmussen, A. Stefani, and O. Bang, "Humidity insensitive TOPAS polymer fiber Bragg grating sensor," Opt. Express **19**(20), 19731–19739 (2011).
12. C. Markos, A. Stefani, K. Nielsen, H. K. Rasmussen, W. Yuan, and O. Bang, "High-Tg TOPAS microstructured polymer optical fiber for fiber Bragg grating strain sensing at 110 degrees," Opt. Express **21**(4), 4758–4765 (2013).
13. A. Stefani, S. Andresen, W. Yuan, N. Herholdt-Rasmussen, and O. Bang, "High sensitivity polymer optical fiber-Bragg-grating-based accelerometer," Photonics Technol. Lett. IEEE **24**(9), 763–765 (2012).
14. C. A. F. Marques, L. B. Bilro, N. J. Alberto, D. J. Webb, and R. N. Nogueira, "Narrow bandwidth Bragg gratings imprinted in polymer optical fibers for different spectral windows," Opt. Commun. **307**, 57–61 (2013).
15. G. D. Peng, Z. Xiong, and P. L. Chu, "Photosensitivity and gratings in dye-doped polymer optical fibers," Opt. Fiber Technol. **5**(2), 242–251 (1999).
16. H. Dobb, D. J. Webb, K. Kalli, A. Argyros, M. C. J. Large, and M. A. van Eijkelenborg, "Continuous wave ultraviolet light-induced fiber Bragg gratings in few- and single-mode microstructured polymer optical fibers," Opt. Lett. **30**(24), 3296–3298 (2005).
17. A. Stefani, C. Markos, and O. Bang, "Narrow bandwidth 850-nm fiber bragg gratings in few-mode polymer optical fibers," IEEE Photon. Technol. Lett. **23**(10), 660–662 (2011).

#230659 - $15.00 USD Received 16 Dec 2014; revised 26 Jan 2015; accepted 28 Jan 2015; published 5 Feb 2015

18. W. Yuan, A. Stefani, M. Bache, T. Jacobsen, B. Rose, N. Herholdt-Rasmussen, F. K. Nielsen, S. Andresen, O. B. Sørensen, K. S. Hansen, and O. Bang, "Improved thermal and strain performance of annealed polymer optical fiber Bragg gratings," Opt. Commun. **284**(1), 176–182 (2011).
19. D. Webb, K. Kalli, and C. Zhang, "Temperature sensitivity of Bragg gratings in PMMA and TOPAS microstructured polymer optical fibres," Proc. Soc. Photo-Optical Instrum. Eng. **6990**, L9900 (2008).
20. I.-L. Bundalo, K. Nielsen, C. Markos, and O. Bang, "Bragg grating writing in PMMA microstructured polymer optical fibers in less than 7 minutes," Opt. Express **22**(5), 5270–5276 (2014).
21. G. D. Marshall, D. J. Kan, A. A. Asatryan, L. C. Botten, and M. J. Withford, "Transverse coupling to the core of a photonic crystal fiber: the photo-inscription of gratings," Opt. Express **15**(12), 7876–7887 (2007).
22. T. Baghdasaryan, T. Geernaert, F. Berghmans, and H. Thienpont, "Geometrical study of a hexagonal lattice photonic crystal fiber for efficient femtosecond laser grating inscription," Opt. Express **19**(8), 7705–7716 (2011).
23. A. Stefani, K. Nielsen, H. K. Rasmussen, and O. Bang, "Cleaving of TOPAS and PMMA microstructured polymer optical fibers: Core-shift and statistical quality optimization," Opt. Commun. **285**(7), 1825–1833 (2012).

1. Introduction

The Fiber Bragg Grating (FBG) technology is a mature technology having applications in numerous devices, most notably in the optical telecommunication sector, but also in the fields of sensing and fiber lasers [1,2]. While the majority of the FBGs have been produced in doped silica fibers [3], in the last decade a lot of research has been put into development of FBGs in polymer optical fibers (POFs). The reason POFs seem a very promising technology is due to various advantages polymers hold over silica, such as higher elastic limit, lower Young's modulus and biological compatibility [4]. These advantages are opening new possibilities in sensing. For example, the higher elastic limit and about 30 times lower Young's modulus of PMMA fibers (2-3 GPa [5–7] with respect to about 72 Gpa in silica [8]) are particularly advantageous when sensing weak forces. Silica fibers can be in general used for up to 1% strain, which is not enough in certain applications, such as in geo-grids and smart textiles [9]. This is where the polymer fibers are preferred as they are less rigid and can be strained up to 10% [8].

PMMA POFs have several downsides such as high transmission loss [10], low glass transition temperature and humidity-temperature cross-sensitivity. While humidity sensitivity can also be used for making humidity sensors, in certain applications that property is unwanted. Humidity sensitivity has been addressed by Yuan et al. where fibers made by the cyclic olefin copolymer called TOPAS [11] have been demonstrated to be insensitive to humidity and also to be capable of operating at higher temperature of up to 120° C [12]. The high losses of POFs do not pose a considerable drawback in applications, such as accelerometers or microphones [13]. However, in order to reduce the losses there is a drive towards making FBGs in the visible spectral window, around 650 nm [14].

Single mode fibers are usually preferred for their accuracy. However, due to doping difficulties when producing single-mode step-index POFs, a lot of research is currently directed towards making microstructured POFs (mPOFs). These fibers are made from a single material having an air-hole microstructured area acting as a lower refractive index cladding and thereby a good control over the index difference enabling endlessly single-mode guidance. FBGs have been written in both step-index [15] and microstructured POFs [16], but the downside of mPOFs is that the air-holes are making it difficult to inscribe gratings as a considerable amount of the incoming inscription laser light is scattered. Exposure times over 60 minutes have been common for 10 mm long gratings in undoped POFs [17–19]. However, recently fast grating inscription in undoped mPOF has been reported, with writing times as low as 6 minutes [20]. In an effort to understand the influence of the microstructured region on the inscription beam, Marshall et *al.* [21] made computational model as well as experiments, where they measured fluorescence from side coupling of laser light to the core of the silica fiber. The results revealed that at certain angles around the angular direction labeled ΓK (see Fig. 1) the coupling to the core was the strongest. Another numerical study was made by T. Baghdasaryan *et al.* [22] focusing on propagation of femtosecond pulses in microstructured fibers, showing very similar results to that of Marshal *et al.* While both studies showed preference for certain angles, a practical study showing formation of the FBGs at different angles is still missing.

#230659 - $15.00 USD Received 16 Dec 2014; revised 26 Jan 2015; accepted 28 Jan 2015; published 5 Feb 2015

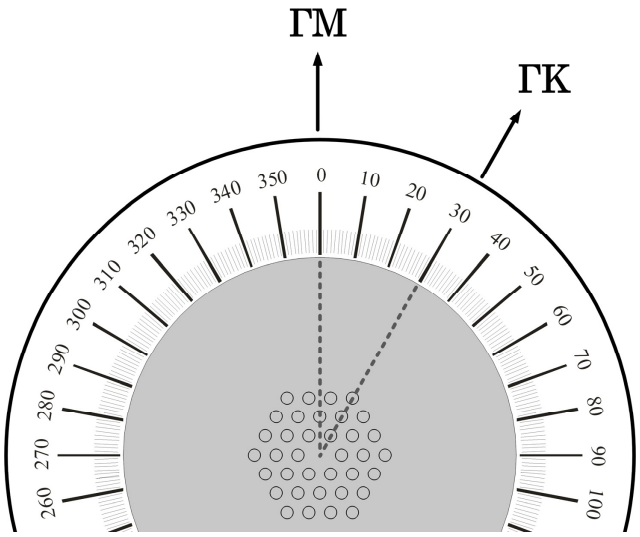

Fig. 1. Microstructured fiber with marked symmetry directions ΓM and ΓK.

2. Inscription setup

The method used for inscription of the FBGs is a standard Phase-mask technique. The laser used for grating inscription is a 30 mW He-Cd CW laser operating at 325 nm by Kimmon (IK5751I-G). The laser output light, which was approximately 3 mm in diameter, was firstly directed through a series of 4 mirrors, one linear polarizer and a focusing lens. The focusing lens was a plano-convex cylindrical lens (Thorlabs LJ4862-UV), which was focusing the incoming laser light through the phase mask down onto the fiber. The phase mask has a uniform pitch of 424.84 nm, a size of 30 mm x 25 mm x 12 mm, it has less than 15% transmission in the 0th order and is custom made by Ibsen Photonics for use with 325 nm light. The fiber, in which the grating is inscribed, is positioned about 100 μm bellow the phase mask.

The FBG interrogation setup consisted of a Supercontinuum white light source from NKT Photonics A/S, an Optical Spectrum Analyzer (OSA, Ando AQ6315A) and an optical spectrometer (Ocean Optics HR2000). An SMF28 pig-tailed silica fiber was used for coupling the light to the mPOF and the light was recorded in reflection through a 3 dB coupler. After the manufacturing of the mPOF there might be some residual stress in the polymer fiber, this stress is released when the fiber is heated [19]. In order to eliminate any issues arising due to the possible heating during the inscription process, fibers are usually annealed prior to inscription. However, the fiber used in this experiment is a non-annealed 3-ring PMMA fiber fabricated at DTU (as presented in [20]), which is endlessly single-moded having a hole to pitch ratio of 0.26 and a hole diameter of 1 μm. The outer diameter of the fiber is approximately 125 μm.

3. Inscription procedure and results

Before the inscription, each mPOF was angle-cleaved to avoid direct reflections back to the detector and was cleaned with alcohol using cleaning tissue. Cleaving was done with a fiber cleaver fabricated in-house [23], where the temperature of both blade and fiber holding plate was set to around 65°C.

The FBG inscription was monitored with an Ocean Optics spectrometer and coupling was continuously optimized with a precision alignment stage so that the FBG reflection peak is observed in spectrum as soon as it forms. Each fiber was irradiated for a total of 30 minutes. The FBG spectrum was monitored in reflection as it grows, and when the growth stopped (observed the same way as shown in [20]), FBG inscription was stopped for a while so that a

#230659 - $15.00 USD Received 16 Dec 2014; revised 26 Jan 2015; accepted 28 Jan 2015; published 5 Feb 2015

high-resolution spectrum could be taken using the OSA. In this first part of the inscription, which is usually finished within 15 min, the physical appearance of the fiber at the position of FBG was seemingly unchanged, but inscription fringes were visible under the microscope as is seen in Fig. 2.

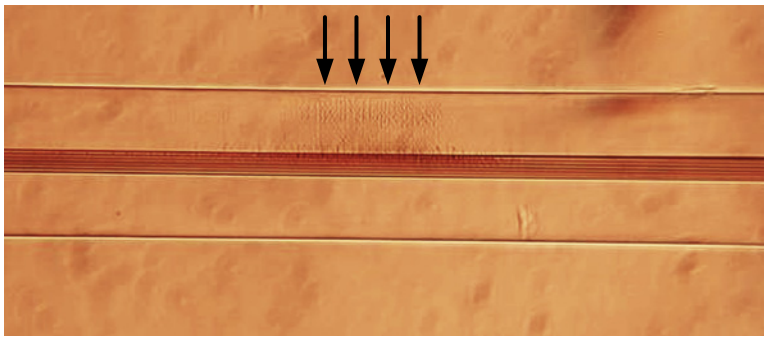

Fig. 2. Fiber with a normal, non-destructive grating visible in the cladding area from above, after 15 minutes of 325 nm UV laser irradiation (arrows are showing the direction of inscription and grating position).

The OSA was used to record the maximum FBG reflection in order to obtain a correct noise floor and peak strength. After the spectrum has been recorded by the OSA, inscription is continued until the total irradiation time was 30 minutes. At that point, the irradiated part of the fiber is burned enough to be clearly visible (see 3 examples in Fig. 3) and the fiber would occasionally even stop guiding.

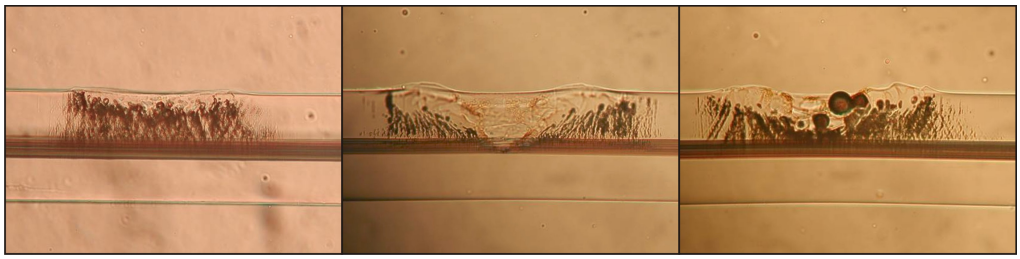

Fig. 3. Fiber after 30 min of 325 nm UV laser FBG inscription on 3 different fiber sections.

The fiber was then removed from the inscription stage and a cleave was made at the position of the FBG. An image was taken of the fiber facet after cleaving. The resulting images are presented in Fig. 4. where the direction of the damaged section, caused by the incident beam, can be seen in relation to the microstructure. Each fiber has been oriented such that the inscription mark is in the upper half of the fiber with one of the ΓM angles pointing up (see Fig. 1). Correspondingly, all the inscription angles lie between the angles 270° (–90°) and 90°.

#230659 - $15.00 USD Received 16 Dec 2014; revised 26 Jan 2015; accepted 28 Jan 2015; published 5 Feb 2015

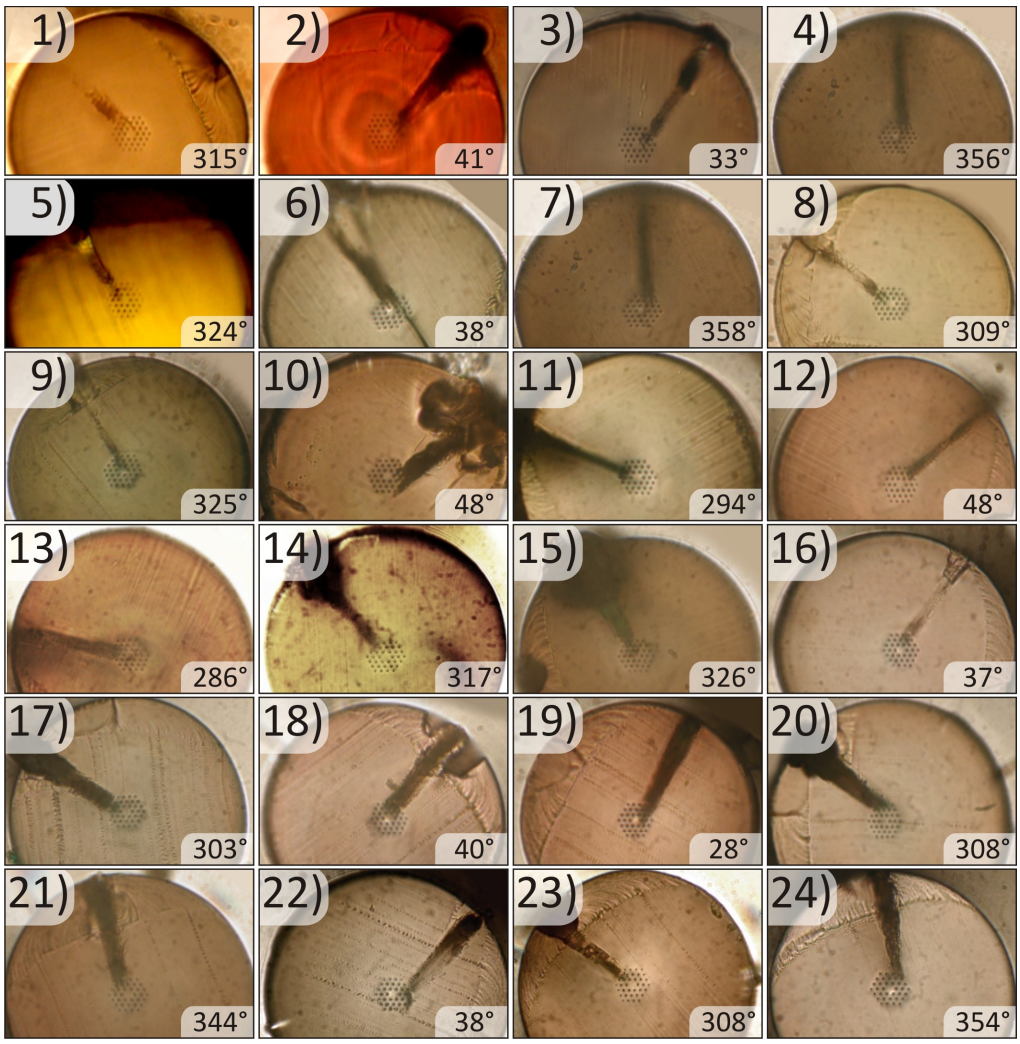

Fig. 4. Fibers and their cross-sections revealing inscription directions when burned with the strong UV laser radiation.

Moreover, due to dihedral (6-fold) and mirror symmetry of the microstructure area, we have mapped all the angles to the 0°-30° range in order to make the angle dependency more clear, as shown in Fig. 5 and Fig. 6. The green lines are FBGs having reflectivity between 12 and 20 dB, orange color is used to map reflectivity of 1-6 dB, while red color is used for fibers not having a visible grating after 30 minutes of inscription. The inscription angle information is presented in the bottom right column of every inset image in the Fig. 4 while consequent mappings with reflection strengths are visible in the Tables 1, Table 2, and Table 3. In the tables we also presented the data regarding the FBG reflection strengths as well as inscription times. Tolerances of the obtained data are 1dB for reading the reflection strengths of the gratings, and 2° for the angles.

#230659 - $15.00 USD Received 16 Dec 2014; revised 26 Jan 2015; accepted 28 Jan 2015; published 5 Feb 2015

Table 1. Fibers with strong gratings (12-20 dB in reflection) after 30 min of FBG inscription. Some gratings have exhibited growths after the first apparent saturation, both times are recorded with the first saturation time in brackets. Fiber numbers refer to Fig. 4.

Fiber No.	**3**	**5**	**9**	**15**	**19**
Original angle	33	324	325	326	28
First 30° angle	27	24	25	26	28
Offset [pitch]	¾ left	¾ right	½ left	0	½ left
FBG reflection	16 dB	16 dB	12 dB	18 dB	19 (7) dB
FBG saturation [min]	/	5.5	9	11	25 (12)

Table 2. a) Fibers with weak gratings (1-6 dB in reflection) after 30 min of FBG inscription. Some gratings have exhibited growths after the first apparent saturation, both times are recorded with the first saturation time in brackets. Fiber numbers refer to Fig. 4.

Fiber No.	**2**	**4**	**6**	**7**	**8**	**13**
Original angle	41	356	322	358	309	286
First 30° angle	19	4	22	2	9	14
Offset [pitch]	1 left	½ left	1 left	½ left	0	0
FBG reflection strength	4 dB	4 dB	6(3) dB	2-3 dB	1-2 dB	5 dB
FBG saturation [min]	/	/	23(15) min	25 min	26 min	23(8) min

Table 2. b) Fibers with weak gratings (1-6 dB in reflection) after 30 min of FBG inscription. Fiber numbers refer to Fig. 4.

Fiber No.	**14**	**16**	**18**	**20 Off center**	**21**	**23**	**24 Off center**
Original angle	317	37	40	308	344	308	354
First 30° angle	17	23	20	8	16	8	6
Offset [pitch]	½ left	½ right	1 right	1½ left	½ right	½ left	1 ½ left
FBG reflection	1-2 dB	3 dB	2 dB	3 dB	1-2 dB	3 dB	2 dB
FBG saturation [min]	20 min	25 min	23 min	15 min	19 min	20 min	20 min

Table 3. Fibers with no gratings after 30 min of FBG inscription. Fiber numbers refer to Fig. 4.

Fiber No.	**1**	**11**	**12**	**17**	**10 Off center**	**22**
Original angle	315°	294°	48°	303°	48°	45°
First 30° angle	15°	6°	12°	3°	12°	15°
Offset [pitch]	0	0	0	½ right	2 left	1 left

It can be seen from the information in tables, Fig. 5 and Fig. 6. that the best angles for the FBG inscription are between 24°-28° as the strongest gratings have been written in that angular region. Those are also the angles closest to ΓK, the angular direction that offers direct access to the core for the laser light.

#230659 - $15.00 USD Received 16 Dec 2014; revised 26 Jan 2015; accepted 28 Jan 2015; published 5 Feb 2015

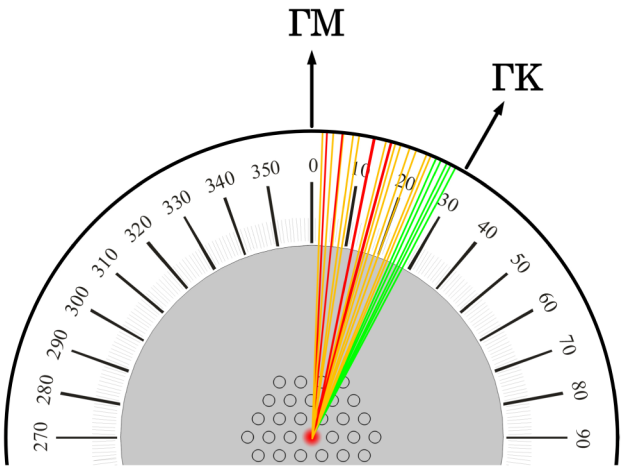

Fig. 5. The microstructure area has a 6-fold symmetry in addition to mirror symmetry of the unit segment which enabled mapping of the inscription angles to the first 30°. Green lines represent fibers having FBG reflectivities of 12-20 dB, orange 1-6 dB, and red represent fibers where no FBG formed in 30 min of inscription.

As the orientation of the fiber on the inscription stage was random, we were unable to obtain information on some angles. Angles 29°-30° were regrettably among those, meaning that we are unable to comment on the simulation results of Marshall *et al.* [21] regarding the decrease of the FBG quality at the ΓK angle. According to their simulation work, the best inscription angles are just around but not exactly at the ΓK angle, while this could not be confirmed with experiments.

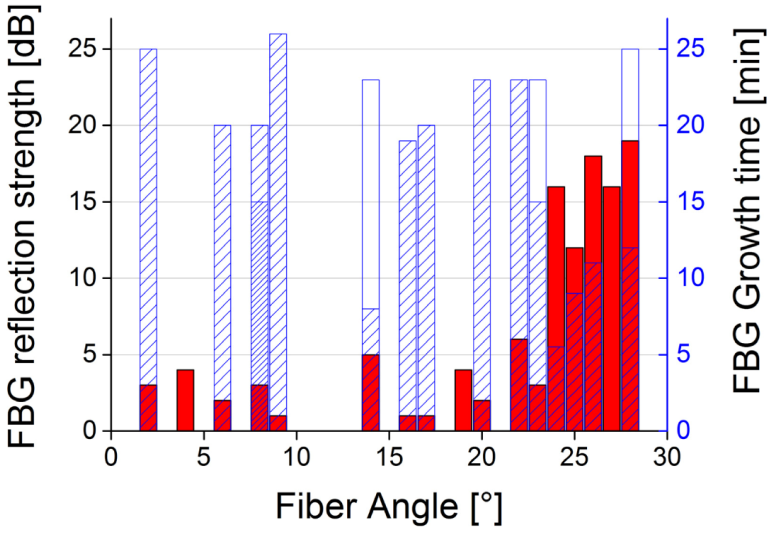

Fig. 6. FBG final grating strengths (red full-color bars) and their corresponding inscription times (blue patterned bars) shown on a bar chart for the mapped 30° angle. For the fibers where FBGs were not written or the inscription time was not recorded there are no blue bars. FBG 13 (14°), 6 (23°) and 19 (28°) experienced two saturations which are depicted with stripped and empty bars. FBGs 20 and 23 (both positioned at 8°) have same strength but their respective inscription times were different. Inscription times were not recorded for the FBGs 2 (19°) and 4 (4°).

#230659 - $15.00 USD Received 16 Dec 2014; revised 26 Jan 2015; accepted 28 Jan 2015; published 5 Feb 2015

In this work we have not dealt with inscription beam offsets due to limited amount of statistical information we could obtain. We assumed that the light completely or partially hitting the core is the light normally forming the grating.

The Fibers having weak gratings (represented by orange color) seem to be evenly distributed over the rest of the angles suggesting that gratings can be obtained from all angles. Fibers without FBGs in them (red) are positioned less than 15° from ΓM, but without clear correlation to draw a conclusion why FBGs have not been formed. Some reasons could be insufficiently cleaned fibers, damage on the fiber surface and, the most probable one being, not enough inscription light reaching the core.

When looking at the speed of inscription, it is clear that the strong gratings (green angles) have been inscribed in short writing times, up to 11 minutes (see Fig. 7). Exceptions are fiber 3 and fiber 19. In fiber 3 (the grating inscribed at 27°) inscription was in the order of 5-10 minutes but the exact duration was not documented. Fiber 19 (the grating inscribed at 28°) exhibited interesting growth, the FBG reflection peak grew and saturated first to 7 dB in 12 minutes, following the spectrum recording, with continued radiation the peak continued to grow slowly but gradually speeding up. In the final 2 minutes of rapid growth, the peak saturated at 19 dB after a total of 25 minutes. Certain other weak FBGs also exhibited similar growth after the apparent first saturation, where the spectrum was taken and inscription was continued. The saturations of those first growths are written in brackets besides the final saturation time in Tables 1, 2, and 3. In Fig. 6, both saturation times are presented for fiber number 19 with blue bars (empty and striped pattern). The saturation time in weak FBGs (orange angles, Table 2) was typically around 19-26 min. It should be noted that those weak FBG peaks were mostly not seen gradually growing but appeared first after longer exposure time, growing up fairly fast until saturation (see Fig. 7).

The reason why good gratings had reflectivity of up to 20 dBs and not more could be due to misalignment of the inscription beam and a fiber.

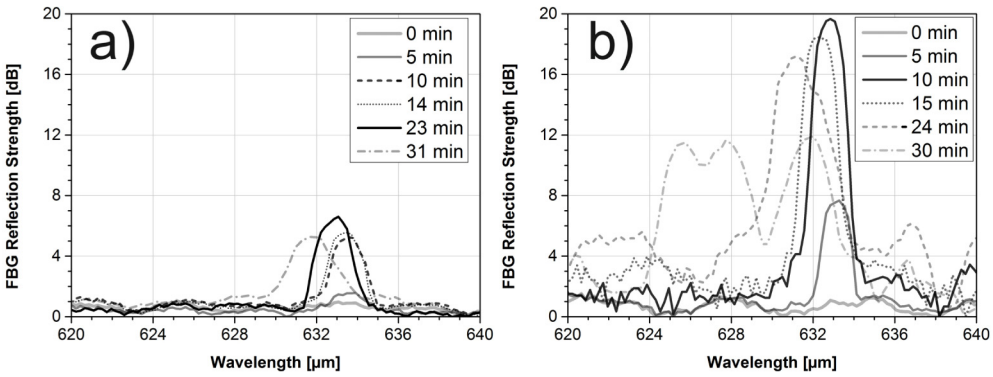

Fig. 7. The FBG reflection spectra showing slower growth of the a) weak grating no. 13 and b) faster growth of the strong grating no. 15 . The growth dynamic of the strong grating (b) shows destruction of the grating after about 30 minutes with the formation of the strong sidepaks while the main peak diminishes. The weak grating has not been destroyed after 30 minutes of irradiation as probably not enough light has entered the core to induce such a destructive change.

One of the interesting formations of FBG can be seen in fibers no. 20 and 24 which had an offset of 1.5 times pitch and, from the images, it is visible that the beam was essentially not hitting the core. However, these two fibers managed to get gratings of 2-3 dBs which is about as strong as other (orange) FBGs. While we do not have enough data to confirm it, this could be due to scattering of the holes where the scattered light still managed to reach the core in sufficient amount to create an index change.

#230659 - $15.00 USD Received 16 Dec 2014; revised 26 Jan 2015; accepted 28 Jan 2015; published 5 Feb 2015

4. Conclusion

Starting from simulation and experiment by Marshall *et al.* we have confirmed their predictions that generally, also in the field of polymer microstructured fibers, the strongest gratings are formed around the certain angles named ΓK. The reason is clearly the direct access of the laser light to the core of the fiber. However, it has also been shown that gratings can be formed from practically any angle hitting the fiber. The condition is that there is enough intensity of the laser light, fiber has a clean surface and there is enough scattering by the holes to the core of the fiber. To get a complete picture of the FBG formation with respect to the power, it would be necessary to repeat the procedure with higher light intensity and better focus. It has been also shown that gratings formed with the laser direction close to ΓK have much faster inscription time and therefore time of saturation. FBGs formed from angles further away from that angle typically start to form after 15 min of irradiation. That time probably varies with inscription light intensity as it has been show in [20]. However, the question still stays unanswered regarding whether with sufficiently high intensity, those (orange) gratings could become also more reflective (order of magnitude of 20 dB), so that we can claim that in high power regime there is no real need for preferred pre-orientation of the fibers.

#230659 - $15.00 USD Received 16 Dec 2014; revised 26 Jan 2015; accepted 28 Jan 2015; published 5 Feb 2015